



Evaluation of Aerial Laser Scanning for fuel mapping in forested ecosystems

And comparison with other fuel inventory methods

Lukas van den Elzen

Degree project/Independent project • 15 credits
Swedish University of Agricultural Sciences, SLU
Southern Swedish Forest Research Centre
BSc Forest and Landscape
Alnarp 2026



Evaluation of Aerial Laser Scanning for fuel mapping in forested ecosystems – and comparison with other fuel inventory methods.

Utvärdering av flyglaserskanning för bränslekartläggning i skogsekosystem – och jämförelse av andra bränsleinventeringsmetoder.

Lukas van den Elzen

Supervisor:	Maksym Matsala, Swedish University of Agricultural Sciences, Southern Swedish Forest Research Centre
Examiner:	Christine Haaland, Swedish University of Agricultural Sciences, Institutionen för landskapsarkitektur, planering och förvaltning
Credits:	15 credits
Level:	Bachelor, G2E
Course title:	Independent project in Landscape Architecture
Course code:	EX1011 40051, VT2026
Programme/education:	BSc Forest and Landscape
Course coordinating dept:	Southern Swedish Forest Research Centre
Place of publication:	Alnarp
Year of publication:	2026
Cover picture:	(if you change the picture on the front page add citation or delete the row)
Copyright:	All featured images are used with permission from the copyright owner/are produced by the author
Keywords:	LiDAR, remote sensing, fuel mapping, fuel inventory, forest fuels, point cloud analysis, understory-monitoring

Swedish University of Agricultural Sciences

Faculty of Forest Sciences

Southern Swedish Forest Research Centre

Abstract

Prescribed burning is a widely used management tool to reduce wildfire hazard, restore (fire-adapted) ecology and enhance ecosystem resilience. Detailed insight into vegetation fuels is crucial for safe and successful controlled burning, but also an important part for understanding ecological processes. After prescribed burning, careful monitoring of ecosystems gives better insight into (post-fire) ecosystem restoration and allows for more direct management. Scientists recognise the potential of remote sensing, and especially LiDAR, for large scale research and monitoring, but empirical comparisons with traditional field-based methods are scarce. This study tried to answer the question whether classification through LiDAR scanning is a reliable and efficient method for mapping fuel composition. Through an experimental setup, point cloud data and orthophotos were gathered from 2 Swedish forests. These were used to train models to classify green fuel coverage and deadwood presence, which were then evaluated based on their reliability and efficiency. The resulting models performed relatively poorly ($F1: 33\text{-}53\%$, $R^2: 21\%$, $RMSE: 12.84$), but the process proved to be efficient. Additionally, a comparison of four other methods (fixed plot, planar intersect, photoload and below-canopy stereophotogrammetry) proved that LiDAR has potential to be the most reliable and efficient method in the right context. Implementing hybrids of methods increases the reliability further, since different methods can compensate for each other's limitations. Overall, this study encourages future studies to test LiDAR with the given methodology and more (diverse) test areas, and highlights the potential of combining LiDAR and field-based approaches for ecological research and monitoring.

Keywords: LiDAR, remote sensing, fuel mapping, fuel inventory, forest fuels, point cloud analysis, understory-monitoring.

Table of contents

List of tables	6
List of figures	7
Abbreviations	8
1. Introduction	9
1.1 Natural fire regimes	9
1.2 Fire behaviour and fuel characteristics	10
1.3 Fuel inventory	11
1.4 Post-fire monitoring	12
1.5 Research objective	13
2. Methods	14
2.1 Methods overview	14
2.2 Study areas	15
2.2.1 Hagestad	15
2.2.2 Alnarp park	16
2.3 Technical equipment	17
2.4 Data collection	17
2.5 Pre-processing	18
2.6 Fuel classification	18
2.7 Modelling	18
2.8 Evaluation of the models	19
2.9 Comparison to other methods	19
3. Results	20
3.1 Orthophotos	20
3.2 ALS and metrics	21
3.2.1 Hagestad	21
3.2.2 Alnarp	22
3.3 Model evaluation	23
3.3.1 Green fuel model	23
3.3.2 Deadwood model	23
3.4 Methods comparison	25
4. Discussion	26
4.1 Model performances	26
4.1.1 Green fuel model	26
4.1.2 Deadwood model	27
4.2 Methods comparison	28
4.2.1 Main findings	28
4.2.2 Synthesis	29

4.3	Methodological limitations	30
4.4	Research implications	30
4.5	Conclusion	31
	References	32
	Appendix A – Flowchart methodology.....	37
	Appendix B – R script classification model	38
	Appendix C – Reference points table.....	39

List of tables

Table 1. The use of different studies for the methods comparison.	19
Table 2. Comparison of the methods FP, PI, PL, BS and LiDAR.	25
Table 3. Table of reference points in Hagestad.	39
Table 4. Table of reference points in Alnarp.	39

List of figures

Figure 1. Map of Scania.	Error! Bookmark not defined.
Figure 2. Map of the Hagestad plot.....	Error! Bookmark not defined.
Figure 3. Map of the Alnarp plot.....	Error! Bookmark not defined.
Figure 4. The Mavic 3M, and Matrice 350 RTK equipped with the Zenmuse L2.....	Error! Bookmark not defined.
Figure 5. Two examples of points in Hagestad.....	Error! Bookmark not defined.
Figure 6. Orthophotos of Hagestad and Alnarp.....	Error! Bookmark not defined.
Figure 7. Metrics plot of Hagestad.....	Error! Bookmark not defined.
Figure 8. Raw point cloud, raster map and understory map of the Hagestad plot.	Error! Bookmark not defined.
Figure 9. Metrics plot of Alnarp.....	Error! Bookmark not defined.
Figure 10. Variable importance plot of HA GF model.....	Error! Bookmark not defined.
Figure 11. Partial dependence plot of HA GF model.....	Error! Bookmark not defined.
Figure 12. Variable importance plot of HA class model.....	Error! Bookmark not defined.
Figure 13. Partial dependence plot of HA class model.....	Error! Bookmark not defined.
Figure 14. Variable importance plot of AL class model.....	Error! Bookmark not defined.
Figure 15. Partial dependence plot of AL class model.....	Error! Bookmark not defined.
Figure 16. The RGB-values of reflective litter and moss. ...	Error! Bookmark not defined.
Figure 17. The RGB-values of deadwood.....	Error! Bookmark not defined.
Figure 18. Flowchart of the methods divided into 'models' and 'comparison'.....	37

Abbreviations

Abbreviation	Description
ALS	Aerial laser scanning
BS	Below-canopy stereophotogrammetry
CWD	Coarse woody debris
DEM	Digital elevation model
DTM	Digital terrain model
FP	Fixed plot method
FWD	Fine woody debris
GCP	Ground control point
GFC	Green fuel coverage
LiDAR	Light detection and ranging
NIR	Near infrared
PI	Planar intersect method
PL	Photoload method
RGB	Red-green-blue spectrum
RTK	Real-time kinematic positioning
SfM	Structure from Motion
UAV	Unmanned aerial vehicle

1. Introduction

1.1 Natural fire regimes

For as long as terrestrial life exists, natural fire regimes have shaped ecosystem structure, successional patterns, and nutrient cycles. Wildfiresⁱ are therefore considered an important source of ecological disturbance in forests, savannas and other environments. (Bowman *et al.*, 2011) During a wildfire environmental processes like biomass accumulation, soil composition, hydrology, carbon exchange and nutrient availability are drastically altered (Sharma *et al.*, 2025). Therefore, wildfires can increase or decrease biodiversity, halt succession, enhance structural complexity, affect animal (meta-)populations, and create ecological niches for fire-dependent species like pyrophilic, saproxylic and pyloporic species (Wikars, 1997; Vanha-Majamaa *et al.*, 2007; Ruokolainen *et al.*, 2009; Engstrom, 2010; Ylisirniö *et al.*, 2012; Thom *et al.*, 2016; Larsson Ekström *et al.*, 2023; Sharma *et al.*, 2025).

In the Anthropocene, the influence of human civilisation has led to large-scale disruption of natural fire regimes on every inhabited continent (Scott *et al.*, 2016; Cogos *et al.*, 2020). Forestry practises add to this trend, because wildfires directly and indirectly threaten production. Despite fire suppression policies (a.k.a. fire exclusion), the number of wildfires increases annually, a phenomenon known as the *wildfire paradox* (Hayes, 2021; Sun *et al.*, 2023), and WWF (2020) reports that 75% of wildfires are directly caused by humans. Fire exclusion also causes accumulation of fuel leading to a higher risk of crown fire and a higher burn intensity (He *et al.*, 2023; Kreider *et al.*, 2024). According to Bowman *et al.* (2009), the increase in the number of wildfires is both increased by, as well as a contributor of, climate change, and the effects of climate change makes forests increasingly susceptible to so-called megafires (Forzieri *et al.*, 2021). A plethora of scientific literature has pointed out the negative effects of a disturbed fire regime on ecosystems (Arshad *et al.*, 2022). For example, the absence of fires can increase successional rates, shorter intervals between fires can disturb natural reproduction of plants and regeneration of ecosystems, and increased fire intensity can lead to higher mortality or even extinction (Kelly *et al.*, 2020). These effects can have cascading effects that threaten already vulnerable species.

ⁱ Wildfire is an umbrella term for any kind of ‘unplanned’ or ‘uncontrolled’ fire in a natural setting. In this paper ‘wildfire’ will be used as a term for a fire-event part of the natural fire regime of that environment.

1.2 Fire behaviour and fuel characteristics

A common method to reduce fire hazard while simultaneously restoring benefits of the natural fire regime is through prescribed burning (Cowman *et al.*, 2021). Additional beneficial effects of prescribed burning are restoration of fire-adapted ecosystems, enhancement of ecosystem resilience, and stimulation of seed germination and regeneration after clearcuts (Eriksson *et al.*, 2013; Clark *et al.*, 2020; Hermanson, 2020; Pereira *et al.*, 2021). Future vegetation composition and soil properties are heavily impacted by the behaviour of the fire (Mitchell *et al.*, 2009; Fonturbel *et al.*, 2021). Long-term this can change ecosystems drastically. Improper burning practices can lead to unforeseen side-effects, like disturbed biodiversity or increased soil erosion (Cawson *et al.*, 2012; Mason *et al.*, 2023).

Fire behaviour (flame length, fire intensity and spread rate) is influenced by three factors: weather, topography and fuel (Biswell, 1999). Of these, fuel is the only governable factor. The fuel type (like green fuel, litter, or woody debris), fuel size (like coarse woody debris (CWD) and fine woody debris (FWD)) and moisture content (higher in green fuels and larger particles) are some of the most important determinants of fire behaviour (Scott *et al.*, 2005; Clark *et al.*, 2020). This study focusses on fuel types ‘green fuels’ (living herbs, moss, lichen) and woody debris of two size classes; CWD (also referred to as ‘deadwood’) and FWD. It is impossible to predict fire behaviour without proper knowledge about the fuel.

Fuel characteristics do not just influence fire behaviour, but also the ecology of a system. Woody debris offers habitat availability for insects, fungi and soil-dwelling organisms. FWD represents the majority of woody debris in managed forests, and important for nutrient cycling and as habitat for many fungi (Brabcová *et al.*, 2022). According to Jonsell *et al.* (2007) FWD is associated with different fungal and beetle species than CWD, and more are dependent on CWD. The amount and diversity of deadwood (CWD) are the largest explanatory variables for polyporic and saproxylic species diversity (Økland *et al.*, 1996). Saproxylic species thrive on niche differentiation, and CWD in different stages of decay offers heterogeneity in dynamic characteristics like porosity, moisture content and nutrient cycling (Parisi *et al.*, 2018; Ruokolainen *et al.*, 2018; Hart *et al.*, 2023). In boreal forests, where saproxylic species account for a significant part of the biodiversity, deadwood retention policies directly lead to fuel accumulation (Larsson *et al.*, 2006; McGeoch *et al.*, 2007). This complicates the relation between fire and biodiversity further, for burning without proper foreknowledge can thus also lead to a decrease of biodiversity. This reinforces the importance of accurate fuel mapping. Detailed information about the fuel is crucial both for safe burning and predictable fire outcomes.

1.3 Fuel inventory

In forest settings, mapping the fuel data can be done in various ways, all with specific strength and limitations. The most implemented methods are field inventories, like fixed plot sampling (FP), planar intersect (PI) and photoload (PL). With the FP, the observer sets up plots of fixed areas in the study area and manually records all the pieces of fuel within its boundaries. It is considered by Arroyo *et al.* (2008) to be the most accurate method, but labour-intensive and prone to misrepresentation. PI is a similar method that counts all the fuel intersecting with a set up line and uses formulas to interpret the fuel load. This works better in heterogeneous terrain, and is very reliable for CWD, but it is also very time-consuming. This limits the ability to implement both FP and PI on large scale. For that reason, methods using photographs, like PL, have been developed since the 1980s (Sikkink *et al.*, 2008). This method estimates fuel characteristics based on reference photographs and is inexpensive and very fast. One problem that all field inventories face is that they rely on samples, which makes them inherently prone to misrepresentation.

Since the late 1970s, remote sensing through satellite imagery has been a tool to analyse the consequences of wildfires and prescribe burning, followed by laser scanning (LiDAR) and use of unmanned aerial vehicles (UAV's) in the early 2010s (Merino *et al.*, 2012; Labenski *et al.*, 2022; Giglio *et al.*, 2024). These methods are usable on large scale and they create spatially continuous data, but mapping fuel through remote sensing techniques is relatively new and empirical evidence on their feasibility is scarce. Abdollahi *et al.* (2025) state that the biggest limiting factors for the use of aerial remote sensing in fuel mapping are their inability to effectively penetrate dense canopies, trouble with interpreting the vertical structure of forests, and costs related to LiDAR data acquisition. A more efficient and reliable method is needed to accurately map forest fuel. An alternative method that addresses the costs and canopy problems is stereophotogrammetry, from drone surveys below the canopy. This method uses a structure from motion (SfM) to create a 3D map from many overlapping photos. The process is relatively fast and cheap, but due to the difficulty of manual flying below-canopy and unreliable georeferencing, feasibility of this method is still unknown (Zhang *et al.*, 2022).

1.4 Post-fire monitoring

After wildfires or prescribed burning, the ecosystem undergoes a complex recovering process that resets succession at least partly. The recovery process can take decades (Kukavskaya *et al.*, 2014) and is dependent on factors before, during and after the fire, like fuel composition, timing, intensity, and climate. Eisenberg *et al.* (2019), for example, observed in Waterton Lakes National Park that two fires with different phenological timings, late spring and late summer, led to a completely different recovery of vegetation. Additionally, occurrence of fires can lead to either positive or negative feedback loops (McLauchlan *et al.*, 2020). Negative feedback stabilises the system, allowing it to recover, but positive feedback makes it more vulnerable to reburning and can lead to irreversible damage (Paritsis *et al.*, 2015; Flores *et al.*, 2024).

The complexity of these recovery processes and increased influence of climate change, add to the importance of post-fire monitoring, both after wildfires and prescribed burning. As field monitoring is often too time- and labour-intensive, remote sensing may be the best alternative, since it is easily scalable (Kurbanov *et al.*, 2022). In addition, repeatability becomes an important factor for post-fire monitoring methods, since areas must be surveyed over long time scales. Most of the remote sensing used in relation to fire today are passive and low resolution (Lopresti *et al.*, 2024). Applications include recognition of spatiotemporal patterns of fire, and fires' impact on air quality. For monitoring vegetation and fuel characteristics, a higher spatial resolution is often needed. Lopresti *et al.* (2024) found that active remote sensing (like LiDAR) is underutilised, but they often perform better than field inventories (Shrestha *et al.*, 2021). Chu *et al.* (2013) state that satellite-based remote sensing is a useful tool for monitoring post-fire recovery and succession, but recovery rates are easily overestimated. Since some species recover faster than others (e.g. herbaceous species vs. woody species), accurate vegetation classification can give more insight into the structural recovery and succession stage of the ecosystem. While optical remote sensing struggles with distinguishing vegetation types (Chu *et al.*, 2016), the ability of LiDAR to measure height and structure, directly addresses this problem.

1.5 Research objective

This project aims to answer the following research questions:

- 1) *Is classification through LiDAR scanning a reliable and efficient method for mapping fuel composition?*
- 2) *Is LiDAR a feasible alternative to traditional field methods?*

Reliability looks at the methods' ability to produce a correct classification and is represented by R^2 (the coefficient of determination), RMSE (root mean square error), accuracy, precision and F1. The *efficiency* is the practical feasibility to implement the methods. This includes the cost of the required equipment, the time needed for fieldwork and data processing, and the proficiency required to operate the drones and software. This project then compares LiDAR scanning and below-canopy stereophotogrammetry to three classic field methods – fixed plot, planar intersect and photoload – also based on *efficiency* and *reliability* as evaluation variables, using existing literature.

The assumption is made that these methods can provide a robust and spatially continuous map of surface fuel types, relatively efficient and more reliable than traditional methods.

2. Methods

2.1 Methods overview

A complete flowchart of the methodology can be found in appendix A. The first drone (*Mavic*) was launched below the canopy for a georeferenced orthophoto. The drone is small and inexpensive but must be operated manually below canopy. The second drone (*Matrice*) was launched for an above-canopy areal laser scanning (ALS), which is fast and produces both optical and structural data, but requires larger and more expensive equipment. These methods were tested in small plots in Hagestad, chosen for the integration of burning in the management, and Alnarp, chosen for its fuel heterogeneity (figure 1). The two plots were made as large as possible without interference of large obstacles like low branches, to increase the amount of usable data. This resulted in a larger plot for Hagestad than for Alnarp.

The types of fuel used for the models are the amount of ‘green fuels’ and the presence of CWD (referred to as ‘deadwood’), since these are important for both fire behaviour and ecological processes. ‘Green fuels’ were analysed as continuous data (0%-100%) and ‘deadwood’ as binary data (0/1). Two non-parametric Random Forest models (regression for green fuels and classification for deadwood) were trained to classify response variables. The models were then evaluated based on their reliability and efficiency and compared to the classic approach of visual examination of surface fuels. For the comparison with other methods, 10 scientific studies were used.



Figure 1. Map of Scania with the two study areas, Alnarp and Hagestad.

2.2 Study areas

2.2.1 Hagestad

The first test area, a 2000 m² oak-pine stand, is located in Hagestad (figure 2), a nature reserve in municipality Ystad in the southeast of Scania. The area is set on quaternary glacial sediments atop limestone from the Cretaceous. The dune landscape is actively influenced by aerial sand drift wherever the ground is not held by vegetation. In the 17th century, the area was covered with scarce oak-scrub forest and heather and was mainly used for grazing. Starting in the early 19th century, the area was covered with scarce oak-scrub forest and heather and was mainly used for grazing. Starting in the early 19th century, pines were planted (*pinus sylvestris* and *pinus nigra*) to prevent erosion. The forest is classified as poor oak on acidic sandy soil (9190), but oak-hornbeam (9160) is also present. The richness of epiphytic species in the oak-scrub forest indicates stability and health. The oak-scrub forest is recognised as ecologically valuable and protected under the birds-and habitats directive of the wider Natura2000 site ‘Sandhammaren’. (Länsstyrelsen, 2014a)

The management of Hagestad tries to create a mosaic landscape with a larger proportion of open areas and more variation between dense and scarce forested areas: 30-70% canopy cover, >20% bare land and 15-30 m³ha⁻¹ deadwood. The open areas will be continuously disturbed and the proportion of deadwood in the forested areas will be increased through thinning, top felling and ringbarking. Länsstyrelsen (2014b) integrated periodic burning into the Hagestad management plan as a long-term measure, but there is no evidence of past burnings. The most recent management plan doesn't justify burning as a measure, but a continually disturbed half-open ecosystem with increased deadwood is their desired outcome.

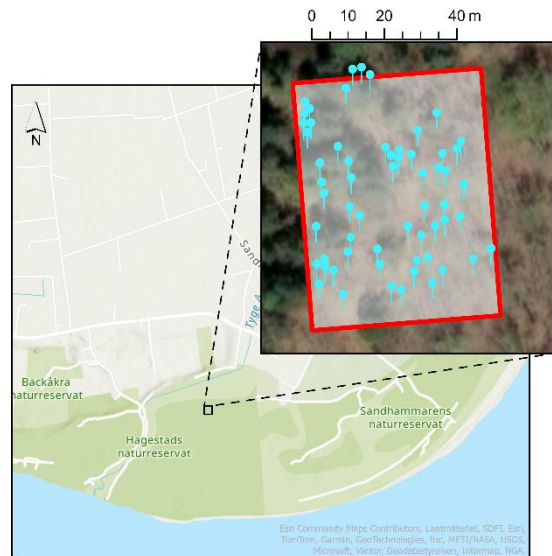


Figure 2. Map of the Hagestad plot with the selected reference points for fuel classification.

2.2.2 Alnarp park

The second test area (900 m²) is located in Alnarpslunden, which is part of Alnarp park (figure 3). It was originally an elm forest but has been replaced by mixed deciduous forest with a rich structural complexity. Ecogain links the long forest continuity and presence of veteran trees to high nature value (Strandberg *et al.*, 2026). Several red-listed species associated with deciduous forests can be found in Alnarpslunden. Apart from its ecological value, Alnarpslunden is valuable for educational, cultural and recreation purposes.

The management is focussed on near-naturalness, but with active intervention against invasive species, diseases and falling branches. Deadwood and high stumps are retained and are considered crucial for the ecological functioning of Alnarpslunden. It is especially beneficial for insects, fungi and soil-dwelling organisms. There is no evidence of pasts burning and it is not mentioned in management plans.



Figure 3. Map of the Alnarp plot with the selected reference points for fuel classification.

2.3 Technical equipment

For the fieldwork, two types of drones were used: A *DJI Mavic 3M* with a multispectral camera for the below-canopy image acquisition, and a *DJI Matrice 350 RTK*, equipped with a *DJI Zenmuse L2* laser scanner, for the above-canopy LiDAR acquisition (henceforth *Mavic*, *Matrice* and *Zenmuse* respectively). The *Mavic* was equipped with *KC586 propeller guards* for drone and operator safety.

Both the *Mavic* (figure 4a) and *Matrice* (figure 4b) have a built-in RTK module with an accuracy of 1-1,5 cm (DJI, n.d.-a). The *Mavic*'s RGB camera has a 20-megapixel 4/3 CMOS sensor, a 24 mm focal length, and a mechanical shutter. The multispectral camera has a 5-megapixel 1/2.8-inch CMOS sensor, a focal length of 25 mm, and an electronic shutter. The multispectral images contain four multispectral bands: green, red, red-edge and near-infrared (G, R, RE and NIR, respectively) (DJI, n.d.-b). The *Zenmuse* supports a point cloud acquisition rate of up to 1.2 million points s^{-1} , with an accuracy of 4-5 cm (DJI, n.d.-c).

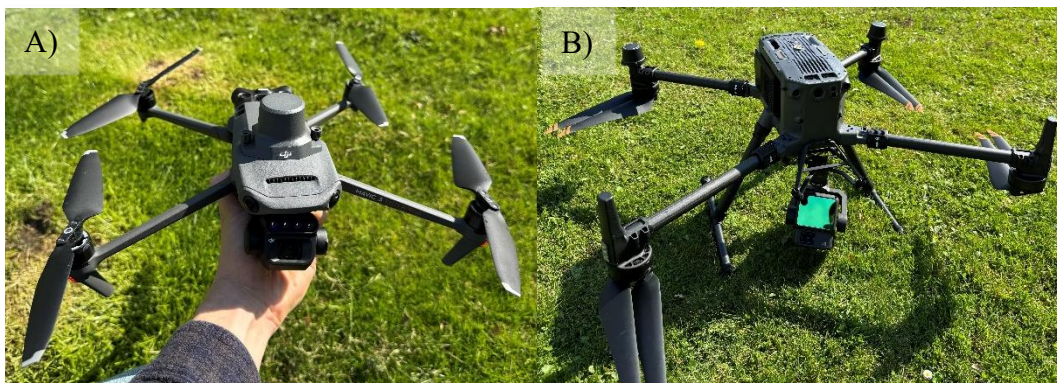


Figure 4. A) The *Mavic 3M* (unfolded: $347.5 \times 283 \times 139.6$ mm) has a weight of 0.95 kg. B) The *Matrice 350 RTK* (unfolded: $810 \times 670 \times 430$ mm), equipped with the *Zenmuse L2*, has a weight of 7.37 kg. Photos by Maksym Matsala.

2.4 Data collection

The data was collected on April 26 (Hagestad) and May 7 (Alnarp), 2026. The plots in Hagestad and Alnarp were roughly 2000 m^2 ($50 \times 40 \text{ m}$) and 900 m^2 ($30 \times 30 \text{ m}$) and manually chosen for their heterogeneity. These plots were uploaded to the *Matrice* as polygons together with local spaceborne DEMs (30m resolution) to create a preplanned flight route. The *Matrice* then executed the automatic above-canopy laser scanning with 80% horizontal and vertical overlap at an altitude of $\sim 35 \text{ m}$. The *Zenmuse* operated in *repetitive scanning mode* for better detection of structures below the canopy and *penta-return recording* to improve the representation of structures closer to the surface. The *Mavic* was used to manually fly below the canopy, while taking vertical photographs (90° angle downward), from an altitude of 3-4 metres above the ground. The *Mavic* took photos at a 2-second interval, while flying with a constant speed of $3,6 \text{ kmh}^{-1}$ (1 ms^{-1}).

2.5 Pre-processing

For the analysis of the data RStudio (R version 4.4) was used with the packages *lidR*, *terra*, and *randomForest* among others (appendix B). The point cloud data was processed identically for Hagestad and Alnarp (HA and AL in the script).

With *DJI Terra*, the photos from the *Mavic* were converted to georeferenced 2D raster orthophotos (TIF format) of surface vegetation with a resolution of 0,1 m.

The ALSs from the *Matrice* were converted to point cloud data (LAS format) with *DJI Terra*. The lowest possible search distance (5 cm) was used to keep a higher point density. The point cloud was normalised by generating DTMs (1-metre resolution) in R and subtracting it from the point cloud. Then, the understory was isolated by slicing the point cloud between 0 and 1 metres above ground level.

2.6 Fuel classification

The orthophotos were used to create a set of manually selected reference points, with focus on an equal distribution of deadwood and green fuel. Within a 1-metre radius of these points two variables were interpreted. *Deadwood*: whether woody debris of >3cm diameter is absent or present (binary data). *Green fuel*: the percentage of the radius covered with living moss, lichens, grass or dwarf shrubs (continuous data). Due to spectral errors in the orthophoto of the Alnarp plot, which caused it to be partly black-and-white, for Alnarp only deadwood was interpreted.

2.7 Modelling

The following six predictor variables were selected from the point cloud data: mean height (zmean), maximum height (zmax), NIR (intensity), red, green, and blue. These were chosen because they may resemble the presence of deadwood, density and complexity of vegetation structures, and the health of green fuels (dead or alive). Higher z (height) values are expected show a positive relationship with deadwood and green fuel, because the height differences are most likely caused by either one. Higher intensity and green likely correlate with green fuels, because chlorophyll reflects green wavelengths and higher moisture contents in healthy plant show a higher reflectivity. Red is reflected more easily by deadwood, due to the brown colouring. Blue may indicate a high level of shade. The six metrics were calculated from the sliced point cloud data for both sites and then rasterised at a resolution of 0,1 metres. The selected reference points from the orthophotos were imported from the Excel files, and a 1-metre buffer was drawn around these points to decrease the effect of high local variability. The mean of the predictor values was calculated for the buffer polygons.

Two non-parametric Random Forest models (regression for green fuels and classification for deadwood) were trained to classify response variables based on the six predictor variables. For the green fuel model (*GF.model*) Random Forest regression was used to model the percentage of green fuel as a continuous response variable. Due to the inability to interpret green fuel from the Alnarp orthophoto, the *GF.model* is only constructed for Hagestad. For the deadwood model (*Class.model*) Random Forest classification was used to predict the presence of deadwood.

2.8 Evaluation of the models

For evaluation of the green fuel models R^2 and RMSE were used, and for the evaluation of the deadwood model the accuracy, precision and F1 were used. Variable importance plots and partial dependence plots were used to interpret the importance of the individual predictor variables for the models. All of the plots shown are generated in Rstudio.

2.9 Comparison to other methods

The five methods – fixed plot (FP), planar intersect (PI), photoload (PL), below-canopy stereophotogrammetry (BS) and LiDAR – were studied using ten studies (table 1). They were then compared using table 2, based on the aforementioned evaluation criteria: reliability and efficiency. The efficiency is subdivided into *labour*, *costs* and *expertise*. Additionally, terms like *scalability* (the ability to use the method on a large scale or in multiple places) and *flexibility* (the ability to make methodological changes) will be taken into account. The reliability is not subdivided, but will summarise criteria used by authors like R^2 , RMSE, accuracy, precision and F1. In addition, the *repeatability* (the ability to repeat the methodology over different spatial or temporal scales) and *representativeness* (the degree of representing the whole study area with the chosen plots/transects). Methods that produce spatially continuous data are thus considered to represent the study area well.

Table 1. The use of different studies for the methods comparison.

Study	FP	PI	PL	BS	LiDAR	Type of study
<i>Behjou et al. (2013)</i>	X	X	X			Original
<i>Borsah et al. (2023)</i>					X	Review
<i>Karjalainen et al. (2026)</i>				X		Original
<i>Keane et al. (2013)</i>	X	X	X			Original
<i>Kramer et al. (2014)</i>	X				X	Original
<i>Lopresti et al. (2024)</i>				X	X	Review
<i>Shimabuku et al. (2023)</i>				X		Original
<i>Sikkink et al. (2008)</i>	X	X	X			Original
<i>Zhang et al. (2022)</i>				X		Original
<i>Zolkos et al. (2013)</i>					X	Review

3. Results

3.1 Orthophotos

The orthophotos of the Hagestad and Alnarp plots varied in quality (figure 6). The Hagestad orthophoto had few parts with sufficient quality for further analysis, due to insufficient overlap and motion blur. The Alnarp orthophoto was higher in quality, but due to technical issues, the photo was largely black-and-white and a large part was missing. Therefore, reference points were selected using only high-quality areas (figure 5), and for Anarp, the green fuel model wasn't used. The reference points and their classifications were saved in Excel tables (see appendix C).

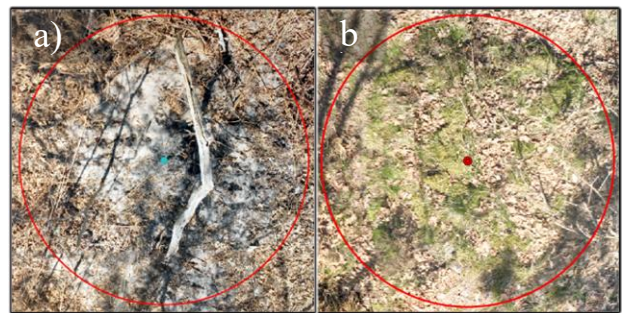


Figure 5. Two examples of points in Hagestad interpreted as a) Shade:0, Deadwood:1, Greenfuel:0, and b) Shade:0, Deadwood:0, Greenfuel:50. The red circles are the 1-metre radius of classification.

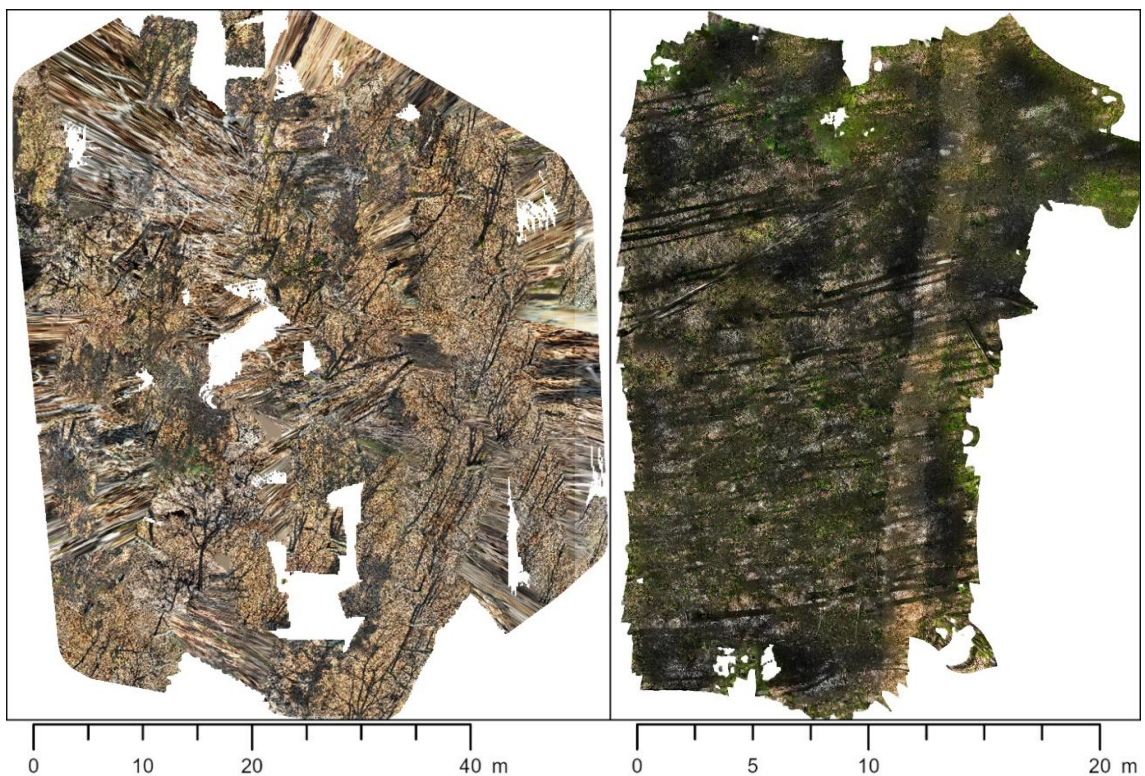


Figure 6. Orthophotos of Hagestad (left) and Alnarp (right) compressed to 330 ppi.

3.2 ALS and metrics

3.2.1 Hagestad

The raw point cloud of Hagestad (figure 7a) contained ~49 million points, of which 25% were classified as ground points and 75% as ‘other’ (vegetation). After rasterisation, normalisation (figure 7b), and slicing, 20% (~9 million) of the points remained for the understory map (figure 7c). Several patches of understory vegetation can be seen, as well as the path in the south-east of the plot.

The metrics plot shows that around the patches of understory vegetation, z_{mean} is a lot lower than z_{max} . This shows the patches are not extremely dense in these places (figure 8).

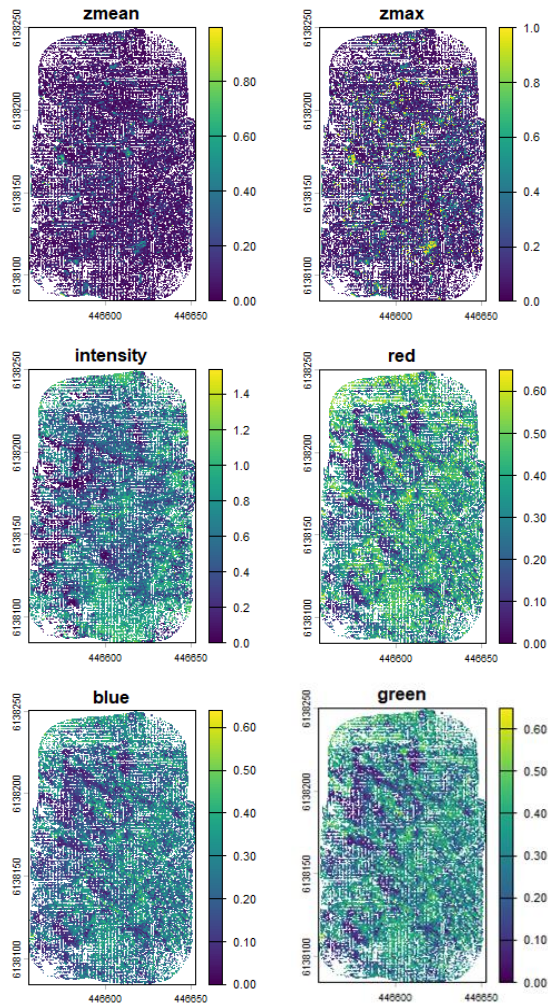


Figure 7. Metrics plot of Hagestad based on the six predictor variables: z_{mean} , z_{max} , intensity, red, blue and green.

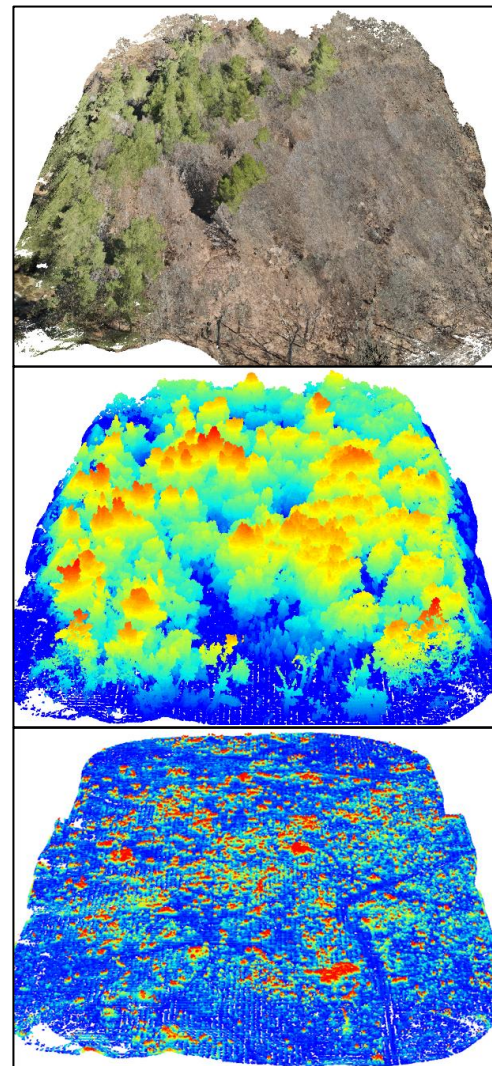


Figure 8. Angled view of the a) raw point cloud in RGB, where the pines are visible in green and the oaks in shades of brown; b) normalised raster map of the Hagestad plot, where the height is visualised in a blue-red colour pallet; and c) understory map of all points between 0 and 1 metres of height (Z).

3.2.2 Alnarp

The metrics plot of Alnarp shows that the height metrics ($zmean$ and $zmax$) are distorted in the north-east corner and south-east edges of the plot (figure 9). The colour values are harder to interpret, but in the same regions where the height is distorted, the colour values are much more homogeneous than in other places. This may indicate faulty data. The data for intensity is missing completely.

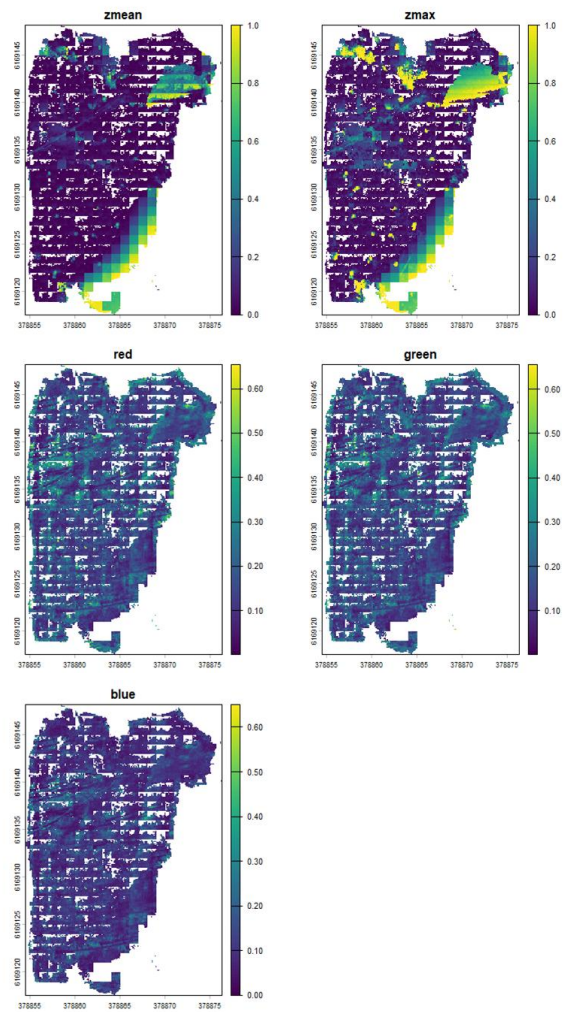


Figure 9. Metrics plot of Alnarp based on five of the six predictor values: $zmean$, $zmax$, red, green and blue.

3.3 Model evaluation

3.3.1 Green fuel model

The green fuel model explained $\sim 21\%$ of the variance of green fuel in Hagestad ($R^2 = 0.21$) with a *RMSE* of 12.84. Despite the relative low performance of the model, the individual predictors show consistent relationships with green fuel predictions. Figure 10 shows that the colour predictors (blue, red, intensity and green) are stronger contributors to the green fuel model, than structural predictors (*zmax*, *zmean* and *CV*). *Blue*, *red* and *green* show similar relations with green fuel; higher values are correlated with lower green fuel predictions. *Intensity* shows more green fuel at low values than high values, with a peak in the low-mid range. *Zmean* and *zmax* show strong negative relations with green fuel predictions; lower height is correlated with a higher green fuel coverage (figure 11).

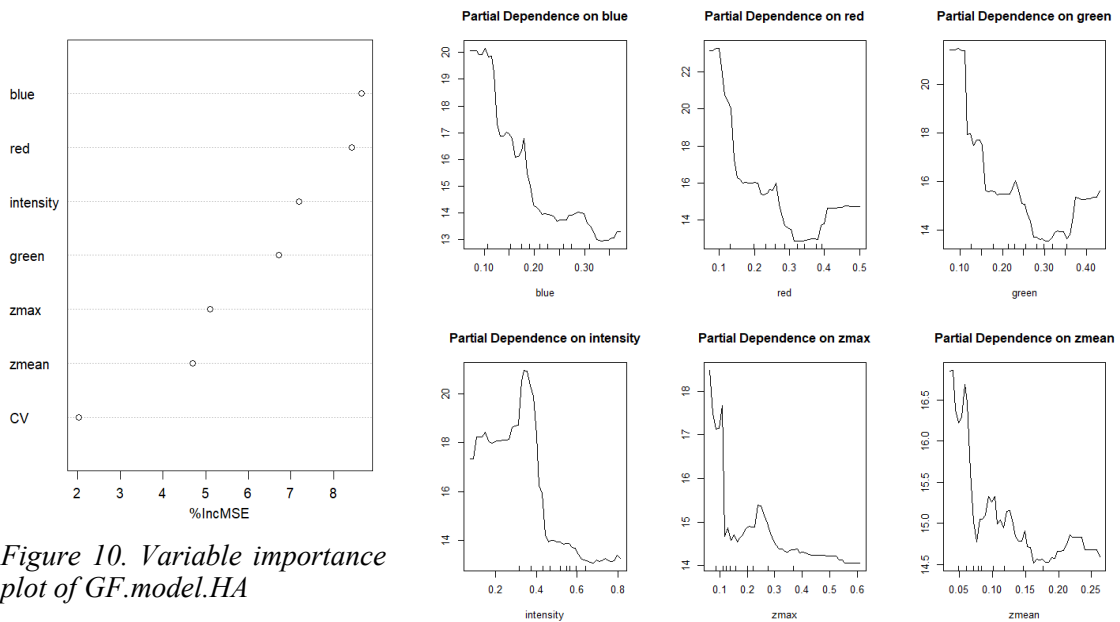


Figure 10. Variable importance plot of GF.model.HA

Figure 11. Partial dependence plot of GF.model.HA containing *zmean*, *zmax*, *red*, *green*, *blue* and *intensity*.

3.3.2 Deadwood model

The deadwood model had moderate predicting power ($FI = 53\%$) and predicted deadwood with an *accuracy* of 61%. Though predictions made are correct 62% of the time (*precision* = 62%), the model missed many instances of deadwood (*recall* = 46%). The model predicted deadwood absence better than presence. Figure 12 shows that *zmean* is the strongest contributor to the deadwood model. *Zmean* and *zmax* showed a positive relationship between height and presence of deadwood, but *Intensity* showed a negative relationship with deadwood presence. *Red*, *green* and *blue* showed a similar parabolic relationship with the presence of deadwood: low and high colour values are correlated with a low chance of deadwood, and middle colour value with a high chance of deadwood (figure 13).

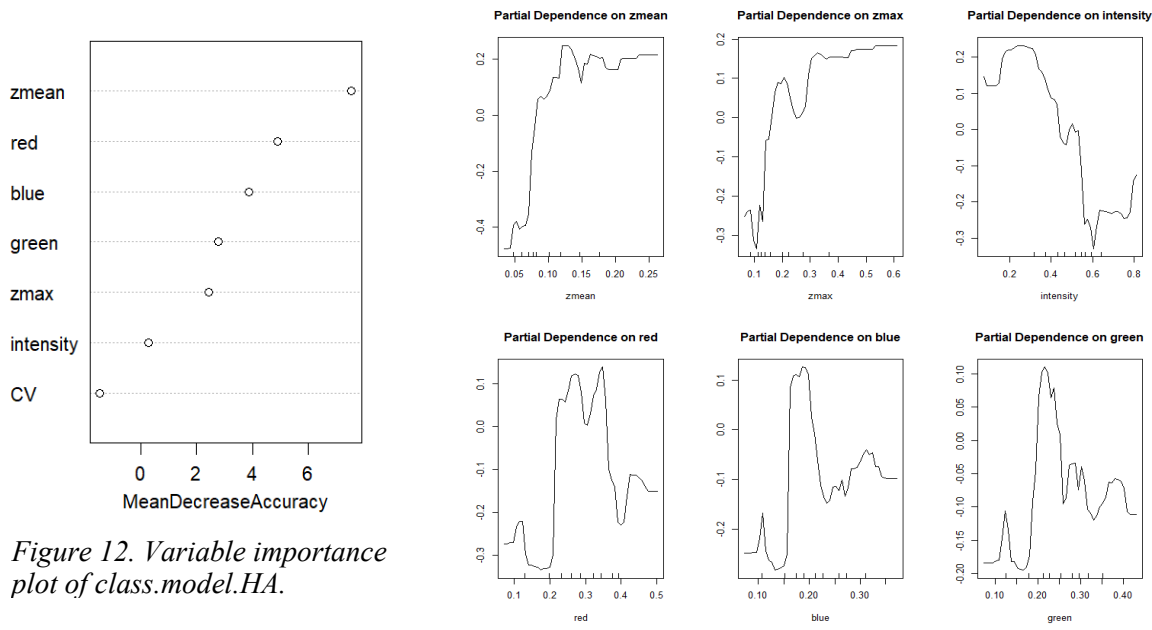


Figure 12. Variable importance plot of class.model.HA.

Figure 13. Partial dependence plot of class.model.HA containing zmean, zmax, red, green, blue and intensity.

Alnarp’s deadwood model had a low predicting power ($F1 = 33\%$). 52% of the total predictions were correct (accuracy = 52%), but there were many false positives (precision = 37%) and false negatives (recall = 30%) were low. This can be explained by an overrepresentation of either class, which the model failed to address. The variable plot shows that each of the separate variables contributes very little to the model’s performance (figure 14). Additionally, the relationship between the independent predictors and the predicted presence of deadwood is marginally different than in Hagestad (figure 15).

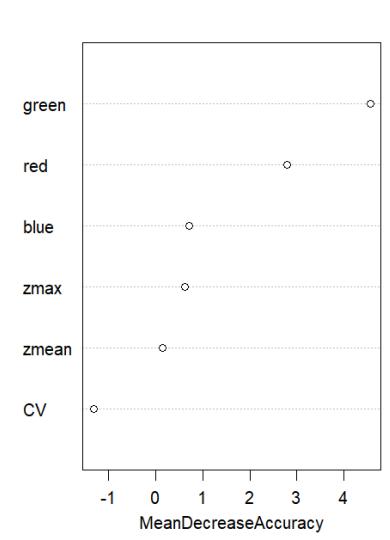


Figure 14. Variable importance plot of class.model.AL

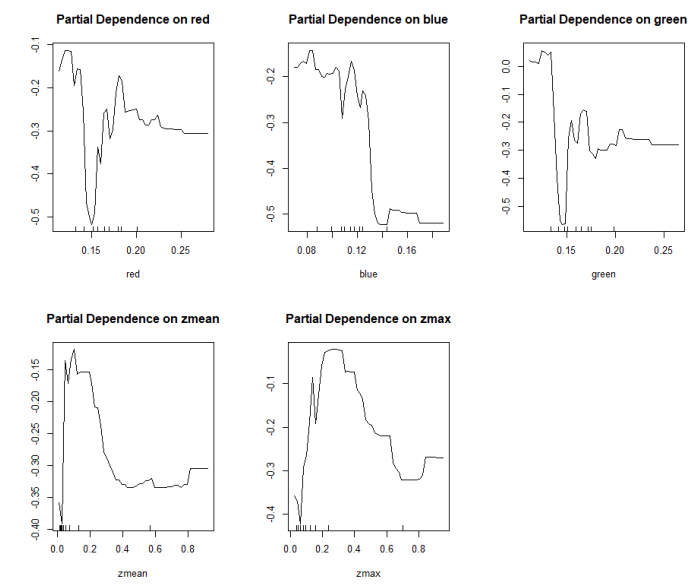


Figure 15. Partial dependence plot of class.model.AL containing zmean, zmax, red, green and blue.

3.4 Methods comparison

Table 2. Comparison of the methods fixed plot, planar intersect, photoload, below-canopy stereophotogrammetry and LiDAR. Overview based on analyses of Behjou et al. (2013), Borsah et al. (2023), Karjalainen et al. (2026), Keane et al. (2013), Kramer et al. (2014), Lopresti et al. (2024), Shimabuku et al. (2023), Sikkink et al. (2008), Zhang et al. (2022) and Zolkos et al. (2012).

<i>Method</i>	<i>Efficiency</i>			<i>Reliability</i>	<i>Evaluation</i>	
	<i>Labour</i>	<i>Costs</i>	<i>Expertise</i>		<i>Strengths</i>	<i>Limitations</i>
<i>Fixed plot</i>	- Very high labour intensity - High variety in efficiency: > Sikkink, 2008: 120 min/ 50 m ² > Behjou, 2013: 60 min/ 400 m ²	- Labour costs - Cheap measuring equipment	- Moderate training required	- High accuracy - Good precision - Unbiased - Good with FWD, less precise with CWD (due to spatial heterogeneity of CWD)	- Very unbiased - Good for FWD classification - Very flexible (good for specific fuel research)	- Very labour intensive - High variety in in operational efficiency - Prone to misrepresentation in heterogeneous sites - Not easily scalable
<i>Planar intersect</i>	- High labour intensity Less variation in efficiency: > Sikkink, 2008: 90 min/ 750 m > Behjou, 2013: 25 min/ 100 m	- Labour costs - Cheap measuring equipment	- Little training required - Methodological consistency is required.	- Most reliable across multiple fields - Good accuracy - Very high precision - Relatively unbiased	- High repeatability - Good for CWD - Better representation in heterogeneous sites	- Labour intensive - Difficult terrain slows efficiency - Bad with complex understory growth - Not easily scalable
<i>Photoload/series</i>	- Low labour intensity - Low/no field time > Sikkink, 2008: ~5 min per photo. > Keane, 2013: “5-25 times faster than PI or FP”	- Labour costs	- Little technical expertise required - Strong influence from interpretation - Extensive training needed for better accuracy	- Least reliable across multiple fields - Low accuracy - High precision (consistent underestimation) - Biased, especially for FWD	- Very quick - Easy and inexpensive - More easily scalable than FP or PI	- Observer bias - Poor repeatability - Bad with FWD
<i>Below-canopy stereophotogrammetry</i>	- Low labour intensity in field: > 30 min/ 0,2 ha ⁱⁱ	- Relatively expensive equipment - Relatively expensive processing software	- High expertise required for manual flight - Moderate expertise for data processing - Drone licence (A1) required in most countries	- High accuracy - Variable precision, (dependant on forest density and operator skill) - Repeatability affected by lighting and image overlap - Relatively unbiased	- Accurate and precise in more open habitats - Low labour intensity - Spatially continuous data reduces sample misrepresentation	- Operator skill required - Reduced visibility from low branches - Less overlap (quality) in dense forests - Large areas need a lot of processing power
<i>LiDAR</i>	- Very low labour intensity in field: > 10 min/ 0,2 ha ⁱⁱ - Large/heavy equipment - Processing is mostly automated	- Very expensive equipment - Very expensive processing software	- High expertise required for flight (pre-planned route) - Moderate expertise for data processing - Drone licence (A2 + STS) required in most countries	- Highest accuracy - Highest precision - Highest repeatability - Minimal bias	- More reliable than field-methods, especially in heterogeneous plots - Low labour intensity - Spatially continuous data reduces sample misrepresentation	- Simplification of complex fuel structures - Expensive equipment makes it inaccessible for small scale research - Large areas need a lot of processing power

ⁱⁱ Estimated time is based on the Mavic/Matrice flight duration in Hagestad, is highly dependent on mission details (point density, photo-overlap, flight altitude), and excludes the (mostly) automated processing procedure.

4. Discussion

4.1 Model performances

4.1.1 Green fuel model

Despite their low to moderate predicting power, the constructed models indicated some trends supported by literature. The green fuel model, based on Hagestad, showed a low performance ($R^2 = 21\%$, $RMSE = 12.84$). For green fuel coverage (GFC), spectral variables contributed more to the model's performance than structural variables. Red, green and blue light reflection showed similar non-linear negative relationships with predicted GFC. For blue and red this is to be expected, since chlorophyll adsorbs blue and red light, these wavelengths are no reflected at higher GFC. However, higher GFC is also associated with more green light reflected, which would show as a positive trend. The nuisance here is that the reflected light is measured on an RGB-spectrum and thus influenced by brightness, not just the spectral characteristics of the vegetation. The darker shades of green fuel in the shade, decrease the reflectance of all colours (figure 16). Another explanation is the influence of bare sand and litter in the Hagestad plot, which strongly reflect *all* wavelengths, and have very low GFC. The model may have learned that high RGB reflection is associated with low GFC and vice versa. The intensity plot shows that in medium NIR-values GFC is predicted to be the highest, because healthy plants reflect more NIR. The high NIR reflection, with low prediction of GFC, can be explained by the influence of bare sand. At low NIR-value the model predicted a moderate amount of GFC, which cannot be explained by low illumination, since LiDAR is an active sensor. An explanation could be that particularly moist or rough green fuels would scatter the light show lower reflection. Though the structural variables contribute less to the model, their independent effect on GFC prediction appears logical. Lower height was associated with more GFC, because most of the green fuels are low-growing mosses and grasses. The jaggedness of the partial dependence plots may indicate the models' instability and overfitting. The model's performance could be increased by a larger sample size, a more equal distribution of GFC classes in the reference points and adding 'shade' as a variable.

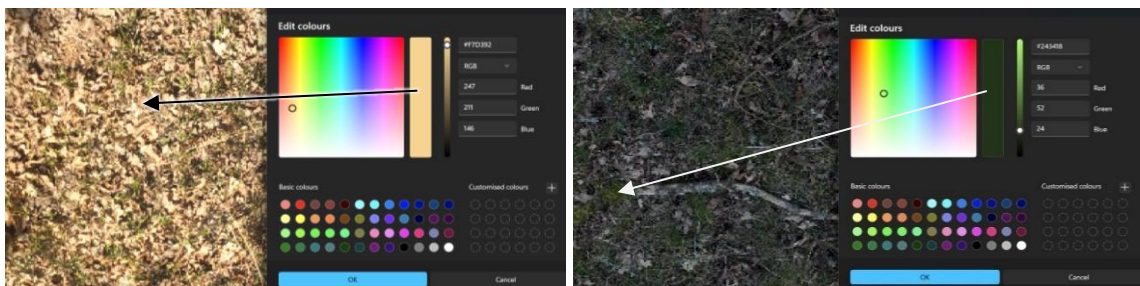


Figure 16. The RGB-values of reflective litter (left) are much higher than that of a patch of moss in the shade (right). The original brightness and colours are shown.

4.1.2 Deadwood model

The deadwood models of Hagestad showed modest performance ($F1 = 53\%$), while Alnarp's model had a low performance ($F1 = 33\%$). The partial dependence plots also showed inconsistency in predictor-response relationship, which could be due to large differences in site heterogeneity and brightness, or the low reliability of the models. The Hagestad model was influenced mostly by the structure. Higher height was associated with high predictions of deadwood presence. In the Hagestad plot, the understory vegetation was mostly low to the ground (mosses and grasses), so deadwood was usually higher than the surrounding vegetation (excluding the trees). Alnarp was more homogeneous in height: there was not much height difference between deadwood and other vegetation. In addition, the height metrics seem especially distorted in the north and south edges of the Alnarp plot (figure 9). Therefore, the height metrics are not reliable in Alnarp's model. Red, green and blue showed similar relationships with the predicted presence of deadwood in Hagestad. Medium colour reflection was associated with high deadwood prediction, while low and high reflection was associated with low deadwood prediction. Like with the green fuel model, the high RGB values are most likely bare sand and reflective litter, low RGB values are green fuel, while the deadwood usual had intermediate RGB values (figure 17). In the Alnarp plot, the individual contribution of colour values to the model is harder to interpret. Generally, the deadwood could be a darker colour than the surrounding vegetation and litter, but due to the low predictive power of the model, it is hard to make assumptions. Like with the green fuel model, the deadwood models' performance could be increased by a larger sample size, a more equal distribution of deadwood in the reference points and adding 'shade' as a variable. This is especially important for heterogeneous sites like Alnarp.

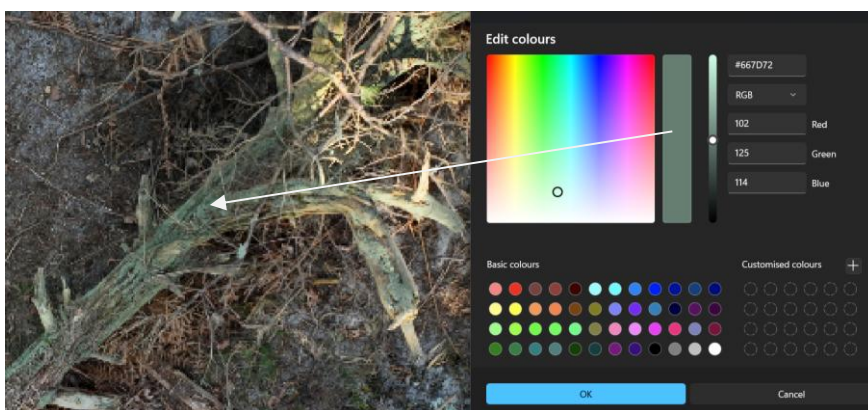


Figure 17. The RGB-values of deadwood are generally more intermediate compared to reflective litter, bare sand or green fuels.

4.2 Methods comparison

4.2.1 Main findings

The comparison of the five methods – fixed plot (FP), planar intersect (PI), photoload (PL), below-canopy stereophotogrammetry (BS) and LiDAR – reveal many strengths and weakness relative to other methods. For mapping and monitoring fuels, the most important factors are reliability (including low bias, high repeatability, good representativeness, etc) and efficiency (including low (variety in) labour intensity, low costs, limited required expertise, high scalability, etc.).

With the FP method, the observer can observe fuel from all sides, operates within clear spatial boundaries, and directly translates fuel observed in the field into data, making this method very unbiased. FP is thus a very reliable method, especially for mapping FWD, but it is the least efficient method. According to multiple studies, FP can take anywhere between 15 and 240 minutes per 100 m², which is the minimum required area to represent a site according to Sikkink *et al.* (2008). This significantly limits the scalability of the method. Additionally, the method struggles with CDW, especially in heterogeneous sites, and is prone to misrepresentation.

PI addresses some of these limitations. PI is also very reliable, and the systematic placement of the lines adds to its repeatability and represents heterogeneous sites better. On top of that, PI is also better at classifying CWD. However, it has the same efficiency problem. The method takes between 90 and 180 minutes per 750 m, the minimum required length to represent a site according to Sikkink *et al.* (2008). The efficiency decreases further in difficult terrain.

PL is the method with the highest efficiency, with only 5 minutes per photo needed. There is no insight given in the required number of photo's per site, but Keane *et al.* (2013) estimate the method to be “5-25 times faster” than PI or FP. This makes it more easily scalable. However, in most reviews, PL performs marginally worse than FP or PI in reliability. It is subjected to systematic bias from the observer unless they are very experienced with the method.

Although not fully validated by existing literature, BS shows potential to be a reliable method because it generates a digital, spatially continuous 3D map of the site which can be interpreted by trained models and AI. BS relies on spatially continuous data, instead of representative sampling. This reduces the risk of sampling bias and allows for better analysis of spatial heterogeneity. The use of models reduces interpretation bias. By using drones in the field and largely automated processing software, this method is efficient: ~30 minutes per 2000 m² in the field. In addition, the maps generated can be used for a multitude of research objectives, and they can be compared to earlier maps for temporal research. The biggest limitations are the expertise and the large processing power required. Additionally, BS struggles with dense forests and complex understory. A lightweight drone like the *Mavic*, and additional processing software like DJI terra are required (currently ~€10.000).

LiDAR is even more efficient than BS, with only ~10 minutes required per 2000 m². It has been shown to have the highest reliability for structural data, while also including optical data, which can be used for a multitude of research objectives. Like BS, it produces spatially continuous data instead of relying on samples. LiDAR's biggest limitations are the required processing power and expensive equipment. A carrier drone like the *Matrice*, laser scanner like the *Zenmuse*, and additional processing software like DJI terra are required (currently ~€40.000).

4.2.2 Synthesis

The historical practice of these five methods shows a trend of gradual automation and increasing reliance on quantitative analyses instead of interpretation in the field. PI is overall considered the best field method by some (Sikkink *et al.*, 2008; Behjou *et al.*, 2013; Keane *et al.*, 2013), but others argue that field methods may soon be largely replaced by better performing remote sensing methods (Shrestha *et al.*, 2021; Kurbanov *et al.*, 2022). Nevertheless, Sikkink *et al.* pose the most relevant statement:

“...choosing one method for use in a sampling program while rejecting others inevitably involves important trade-offs between accuracy, time, money, training, scale, and effectiveness.”

An actual comparison of method depends mostly on the context of the research. FP and PI are both very flexible, since very little material is needed, and the time required for good reliability drastically decreases when only specific types of fuel need to be researched. In addition, personal field visits give researchers the ability to observe the whole site and gain a better ecological insight into the study area. FP could be the best method for accurate FWD examinations in one forest, while PI could be the best for CWD inventories in heterogeneous forests. For a quick analysis spanning many different sites, where high accuracy isn't the priority, PL would be the best method. BS would be a promising method for fuel mapping before prescribed burning, because it can create a continuous map of the forest floor without much labour. For the monitoring of a large area, where many variables are taken into account, LiDAR would be the best method, because with repeated surveys, ecological processes can be distinguished. When research asks for it, strategic combinations between methods can address limitations of singular methods. As shown in the results chapter, LiDAR data can become distorted due to occultation, faulty interpolations or other errors. Field methods can complement remote sensing methods by manually checking areas with distortions or missing data. For a large project, PL can be used for a general survey, BS or LiDAR can be used for spatial mapping and FP or PI can be implemented in specific sites of interest. Recognising methodological strengths and limitations is crucial for any scientific research.

4.3 Methodological limitations

Despite logical interactions between the metric variables and the models' performance, the models' reliability was low compared to many published experiments. This can largely be attributed to the small sample size, limited parameters involved and a plethora of technical and logistical setbacks. Due to scheduling issues many of these setbacks were resolved by changing the methodology, instead of repeating the field work, up until several days before the deadline.

One major change to the methodology was the removal of below-canopy stereophotogrammetry (BS) from the experimental part of the study. Part of the methodology was the use of an RTK pole for ground control points (GCPs), to achieve a high georeference-precision. However, last minute it became unavailable, forcing us to use a Garmin GPS device as an alternative. During the tests of the BS-models, the device turned out to lack the precision for accurate pixel classification of the orthophotos, and decreasing the resolution led to insufficient proving power for the prediction model. Since precise georeferencing was crucial for this method, it was removed, changing focus to LiDAR data. For this method, the orthophoto could still be used for visual interpretation or manually selected reference points. However, this method led to additional bias due to manual point selection.

Due to hardware issues, the LiDAR data of the second study area (Alnarp) was only generated several days before the deadline. To prepare for potential problems with the data of Alnarp, a comparison between other methods was prepared as a back-up. When the data indeed turned out to be incomplete and partly distorted, this comparison was developed. Due to time constraints the comparison was less extensive than it could have been, with only ten used studies. Of these, three were reviews, and they all concerned LiDAR. A larger number of studies, along with a more equal distribution of original research and reviews, would improve the comparison of methods.

4.4 Research implications

This study has shown the relevance of careful methodological selection and possibly combination of fuel inventory and monitoring methods. Researchers are encouraged to make use of all available technologies, classic and modern, to improve on their research. The experimental design of the LiDAR based fuel models leaves a lot of room for improvement. To increase the performance of all models, this study could be repeated with a consistent, preplanned methodology, and more suitable research areas with heterogeneous fuels. The increased amount of data will increase the reliability of the models and reduce the impact of technical issues.

Additionally, this study contributes to the growing body of literature evaluating the advantages and limitations of LiDAR for ecological research and monitoring. Other literature describes LiDAR as a reliable and efficient method and recognises its increasing role in research. Even though the models in this study showed little statistical significance, the study's workflow proves LiDAR's efficiency. Hence, this study recognises the potential to use LiDAR on a large scale for ecological research.

4.5 Conclusion

This project aimed to evaluate the potential of fuel classification through LiDAR scanning and how it compares to other fuel inventory methods. This study found that LiDAR shows promise to be used efficiently, and possibly in combination with other methods, to generate reliable data that can be used for a wide range of applications. In addition, LiDAR produces spatially continuous data that can represent heterogeneous areas better than samples can. The effectiveness depends mostly on the research objectives and context. The green fuel and deadwood models used for testing the reliability of LiDAR in fuel mapping performed relatively poorly, which can be attributed to methodological flaws and a small sample size. Nevertheless, the models showed logical relationships between individual values and fuel predictions. Spectral values appeared to be the strongest contributor to the green fuel model, while structural values were important for the deadwood model. Other literature has produced some empirical evidence that suggests LiDAR has the potential to be more accurate, precise and unbiased than traditional field methods. The implementation of LiDAR proved reasonably time-efficient, with only 10 minutes needed in the field, and the processing being largely automated. This makes it much more efficient than fixed plot or planar intersect methods. The required training and equipment are very expensive, however, which reduces the applicability for small scale research. Using below-canopy stereophotogrammetry could bridge the gap by producing continuous orthophotos or 3D maps with a relatively inexpensive drone. Overall, field methods are labour-intensive, but reliable and flexible. And while remote sensing methods are technologically demanding, they are easily scalable and produce spatially continuous data. Choosing any one method usually involves trade-offs, therefore hybrid methods can be highly valuable depending on the context. In the near future, automation, AI, and better accessibility to remote sensing will likely change ecological research drastically. With remote sensing becoming increasingly important in science, understanding its strengths and drawbacks is crucial for effective application.

References

- Abdollahi, A., & Yebra, M. (2025). *Challenges and Opportunities in Remote Sensing-Based Fuel Load Estimation for Wildfire Behavior and Management: A Comprehensive Review*. *Remote Sensing*, 17(3), 415.
- Arroyo, L. A.; Pascual, C., & Manzanera, J. A. (2008). *Fire models and methods to map fuel types: The role of remote sensing*. *Forest Ecology and Management*, 256(6), 1239-1252.
<https://doi.org/10.1016/j.foreco.2008.06.048>
- Arshad, A.; Azhar, A., & Anjali, K. (2022). *Impact of Forest Fire on Forest Ecosystem*.
- Behjou, F., & Mollabashi, O. G. (2013). *Assessment of coarse woody debris following selective logging in Caspian forests: implications for conservation and management*. *Journal of Forest Science*, 59, 117-124.
<https://doi.org/10.17221/78/2012-JFS>
- Biswell, H. H. (1999). *Prescribed Burning in California Wildlands Vegetation Management* (1 ed.). University of California Press.
<https://doi.org/10.2307/jj.8501326>
- Bowman, D.; Balch, J.; Artaxo, P., et al. (2009). *Fire in the Earth System*. *Science* (New York, N.Y.), 324, 481-484. [10.1126/science.1163886](https://doi.org/10.1126/science.1163886)
- Bowman, D. M. J. S.; Balch, J.; Artaxo, P., et al. (2011). *The human dimension of fire regimes on Earth*. *Journal of Biogeography*, 38(12), 2223-2236.
<https://doi.org/10.1111/j.1365-2699.2011.02595.x>
- Brabcová, V.; Tlaskal, V.; Lepinay, C., et al. (2022). *Fungal Community Development in Decomposing Fine Deadwood Is Largely Affected by Microclimate*. *Frontiers in Microbiology*, 13, 835274.
<https://doi.org/10.3389/fmicb.2022.835274>
- Cawson, J. G.; Sheridan, G. J.; Smith, H. G., et al. (2012). *Surface runoff and erosion after prescribed burning and the effect of different fire regimes in forests and shrublands: a review*. *International Journal of Wildland Fire*, 21(7), 857-872. <https://doi.org/10.1071/WF11160>
- Chu, T., & Guo, X. (2013). *Remote Sensing Techniques in Monitoring Post-Fire Effects and Patterns of Forest Recovery in Boreal Forest Regions: A Review*. *Remote Sensing*, 6. <https://doi.org/10.3390/rs6010470>
- Chu, T.; Guo, X., & Takeda, K. (2016). *Remote sensing approach to detect post-fire vegetation regrowth in Siberian boreal larch forest*. *Ecological Indicators*, 62, 32-46. <https://doi.org/10.1016/j.ecolind.2015.11.026>
- Clark, K.; Heilman, W.; Skowronski, N., et al. (2020). *Fire Behavior, Fuel Consumption, and Turbulence and Energy Exchange during Prescribed Fires in Pitch Pine Forests*. *Atmosphere*, 11, 242.
<https://doi.org/10.3390/atmos11030242>
- Cogos, S.; Roturier, S., & Östlund, L. (2020). *The origins of prescribed burning in Scandinavian forestry: the seminal role of Joel Wretling in the management of fire-dependent forests*. *European Journal of Forest Research*, 139(3), 393-406. <https://doi.org/10.1007/s10342-019-01247-6>

- Cowman, D., & Russell, W. (2021). *Fuel load, stand structure, and understory species composition following prescribed fire in an old-growth coast redwood (Sequoia sempervirens) forest*. *Fire Ecology*, 17(1), 17. <https://doi.org/10.1186/s42408-021-00098-0>
- DJI. (n.d.-a). *Matrice 350 RTK – Specs*. DJI Enterprise. Retrieved April from <https://enterprise.dji.com/matrice-350-rtk/specs>
- DJI. (n.d.-b). *Mavic 3 Multispectral – Specs*. DJI Enterprise. Retrieved April from <https://enterprise.dji.com/mavic-3-m/specs>
- DJI. (n.d.-c). *Zenmuse L2 – Specs*. DJI Enterprise. Retrieved April from <https://enterprise.dji.com/zenmuse-l2/specs>
- Eisenberg, C.; Anderson, C. L.; Collingwood, A., et al. (2019). *Out of the Ashes: Ecological Resilience to Extreme Wildfire, Prescribed Burns, and Indigenous Burning in Ecosystems* [Original Research]. *Frontiers in Ecology and Evolution*, Volume 7 - 2019. <https://doi.org/10.3389/fevo.2019.00436>
- Engstrom, R. T. (2010). *First-Order Fire Effects on Animals: Review and Recommendations*. *Fire Ecology*, 6(1), 115-130. <https://doi.org/10.4996/fireecology.0601115>
- Eriksson, A.-M.; Olsson, J.; Jonsson, B., et al. (2013). *Effects of restoration fire on dead wood heterogeneity and availability in three Pinus sylvestris forests in Sweden*. *Silva Fennica*, 47, 1-15. <https://doi.org/10.14214/sf.954>
- Flores, B. M.; Montoya, E.; Sakschewski, B., et al. (2024). *Critical transitions in the Amazon forest system*. *Nature*, 626(7999), 555-564. <https://doi.org/10.1038/s41586-023-06970-0>
- Fonturbel, T.; Carrera Pérez, N.; Vega, J., et al. (2021). *The Effect of Repeated Prescribed Burning on Soil Properties: A Review*. *Forests*, 12, 767. <https://doi.org/10.3390/f12060767>
- Forzieri, G.; Girardello, M.; Ceccherini, G., et al. (2021). *Emergent vulnerability to climate-driven disturbances in European forests*. *Nature Communications*, 12(1), 1081. <https://doi.org/10.1038/s41467-021-21399-7>
- Giglio, L., & Justice, C. O. (2024). *Early polar-orbiting satellite-based fire remote sensing during the 1960s*. *International Journal of Remote Sensing*, 45(16), 5605-5615. <https://doi.org/10.1080/01431161.2024.2377838>
- Hart, S.; Porter, T.; Basiliko, N., et al. (2023). *Fungal community dynamics in coarse woody debris across decay stage, tree species, and stand development stage in northern boreal forests*. *Canadian Journal of Forest Research*, 54. <https://doi.org/10.1139/cjfr-2023-0061>
- Hayes, J. P. (2021). *Fire Suppression and the Wildfire Paradox in Contemporary China: Policies, Resilience, and Effects in Chinese Fire Regimes*. *Human Ecology*, 49(1), 19-32. <https://doi.org/10.1007/s10745-020-00183-z>
- He, H.; Chang, Y.; Liu, Z., et al. (2023). *Evaluations on the Consequences of Fire Suppression and the Ecological Effects of Fuel Treatment Scenarios in a Boreal Forest of the Great Xing'an Mountains, China*. *Forests*, 14(1), 85.
- Hermanson, V. C. (2020). *Prescribed Burning in Sweden – An Evaluation of Structural Outcomes from Restoration Oriented Prescribed Burns* [Swedish University of Agricultural Sciences]. Uppsala.

- Jonsell, M.; Hansson, J., & Wedmo, L. (2007). *Diversity of saproxylic beetle species in logging residues in Sweden – Comparisons between tree species and diameters*. *Biological Conservation*, 138(1), 89-99. <https://doi.org/10.1016/j.biocon.2007.04.003>
- Keane, R., & Gray, K. (2013). *Comparing three sampling techniques for estimating fine woody down dead biomass*. *International Journal of Wildland Fire*, 22, 1093-1107. <https://doi.org/10.1071/WF13038>
- Kelly, L.; Giljohann, K.; Duane, A., et al. (2020). *Fire and biodiversity in the Anthropocene*. *Science*, 370, eabb0355. <https://doi.org/10.1126/science.abb0355>
- Kreider, M. R.; Higuera, P. E.; Parks, S. A., et al. (2024). *Fire suppression makes wildfires more severe and accentuates impacts of climate change and fuel accumulation*. *Nature Communications*, 15(1), 2412. <https://doi.org/10.1038/s41467-024-46702-0>
- Kukavskaya, E. A.; Ivanova, G. A.; Conard, S. G., et al. (2014). *Biomass dynamics of central Siberian Scots pine forests following surface fires of varying severity*. *International Journal of Wildland Fire*, 23(6), 872-886. <https://doi.org/10.1071/WF13043>
- Kurbanov, E.; Vorobev, O.; Lezhnin, S. A., et al. (2022). *Remote Sensing of Forest Burnt Area, Burn Severity, and Post-Fire Recovery: A Review*. *Remote Sensing*, 14, 4714. <https://doi.org/10.3390/rs14194714>
- Labenski, P.; Ewald, M.; Schmidlein, S., et al. (2022). *Classifying surface fuel types based on forest stand photographs and satellite time series using deep learning*. *International Journal of Applied Earth Observation and Geoinformation*, 109, 102799. <https://doi.org/10.1016/j.jag.2022.102799>
- Länsstyrelsen. (2014a). *Beslut om bildande av naturreservatet Hagestad i Ystad kommun*. (511-12818-2014). Malmö Sweden: Länsstyrelsen Skåne
- Länsstyrelsen. (2014b). *Skötselplan för naturreservatet Hagestad – Ystad kommun, Skåne län*.
- Larsson Ekström, A.; Sjögren, J.; Djupström, L. B., et al. (2023). *Reinventory of permanent plots show that kelo lichens face an extinction debt*. *Biological Conservation*, 288, 110363. <https://doi.org/10.1016/j.biocon.2023.110363>
- Larsson, S.; Ekbom, B.; Schroeder, M., et al. (2006). *Saproxylic beetles in a Swedish Boreal forest landscape managed according to 'new forestry'*.
- Lopresti, A.; Hayden, M.; Siegel, K., et al. (2024). *Remote sensing applications for prescribed burn research*. *International Journal of Wildland Fire*, 33. <https://doi.org/10.1071/WF23130>
- Mason, S. C.; Shirey, V.; Waite, E. S., et al. (2023). *Exploring Prescribed Fire Severity Effects on Ground Beetle (Coleoptera: Carabidae) Taxonomic and Functional Community Composition*. *Fire*, 6(9), 366.
- McGeoch, M. A.; Schroeder, M.; Ekbom, B., et al. (2007). *Saproxylic beetle diversity in a managed boreal forest: importance of stand characteristics and forestry conservation measures*. *Diversity and Distributions*, 13(4), 418-429. <https://doi.org/10.1111/j.1472-4642.2007.00350.x>
- McLauchlan, K. K.; Higuera, P. E.; Miesel, J., et al. (2020). *Fire as a fundamental ecological process: Research advances and frontiers*. *Journal of Ecology*, 108(5), 2047-2069. <https://doi.org/10.1111/1365-2745.13403>

- Merino, L.; Caballero, F.; Martinez-de Dios, J. R., et al. (2012). *An Unmanned Aircraft System for Automatic Forest Fire Monitoring and Measurement*. *Journal of Intelligent and Robotic Systems*, 65, 533-548.
<https://doi.org/10.1007/s10846-011-9560-x>
- Mitchell, R. J.; Hiers, J. K.; O'Brien, J., et al. (2009). *Ecological Forestry in the Southeast: Understanding the Ecology of Fuels*. *Journal of Forestry*, 107(8), 391-397. <https://doi.org/10.1093/jof/107.8.391>
- Økland, B.; Bakke, A.; Hågvar, S., et al. (1996). *What factors influence the diversity of saproxylic beetles? A multi-scale study from a spruce forest in southern Norway*. *Biodiversity and Conservation*, 5, 75-100.
<https://doi.org/10.1007/BF00056293>
- Parisi, F.; Pioli, S.; Lombardi, F., et al. (2018). *Linking deadwood traits with saproxylic invertebrates and fungi in European forests - a review*. *iForest - Biogeosciences and Forestry*, 11, 423-436.
<https://doi.org/10.3832/ifor2670-011>
- Paritsis, J.; Veblen, T. T., & Holz, A. (2015). *Positive fire feedbacks contribute to shifts from *Nothofagus pumilio* forests to fire-prone shrublands in Patagonia*. *Journal of Vegetation Science*, 26(1), 89-101.
<https://doi.org/10.1111/jvs.12225>
- Pereira, P.; Bogunovic, I.; Zhao, W., et al. (2021). *Short term effect of wildfires and prescribed fires on ecosystem services*. *Current Opinion in Environmental Science & Health*, 22, 100266. <https://doi.org/10.1016/j.coesh.2021.100266>
- Ruokolainen, A.; Shorohova, E.; Penttilä, R., et al. (2018). *A continuum of dead wood with various habitat elements maintains the diversity of wood-inhabiting fungi in an old-growth boreal forest*. *European Journal of Forest Research*, 137(5), 707-718. <https://doi.org/10.1007/s10342-018-1135-y>
- Ruokolainen, L., & Salo, K. (2009). *The Effect of Fire Intensity on Vegetation Succession on a Sub-Xeric Heath during Ten Years after Wildfire*. *Annales Botanici Fennici*, 46, 30-42. <https://doi.org/10.5735/085.046.0103>
- Scott, A. C.; Chaloner, W. G.; Belcher, C. M., et al. (2016). *The interaction of fire and mankind: Introduction†*. *Philosophical Transactions of the Royal Society B: Biological Sciences*, 371(1696), 20150162.
<https://doi.org/10.1098/rstb.2015.0162>
- Scott, J. H., & Burgan, R. E. (2005). *Standard fire behavior fuel models: a comprehensive set for use with Rothermel's surface fire spread model*. <http://dx.doi.org/10.2737/RMRS-GTR-153>
- Sharma, S. K., & Kumar, K. (2025). *Forest Fire Effects on Structure, Composition, and Functioning of Ecosystem*. In H. Singh, et al. (Eds.), *Forest Fire and Climate Change: Insights into Science* (pp. 79-99). Springer Nature Switzerland. https://doi.org/10.1007/978-3-031-89967-6_5
- Shrestha, M.; Broadbent, E. N., & Vogel, J. G. (2021). *Using GatorEye UAV-Borne LiDAR to Quantify the Spatial and Temporal Effects of a Prescribed Fire on Understory Height and Biomass in a Pine Savanna*. *Forests*, 12(1), 38.
- Sikkink, P., & Keane, R. (2008). *A comparison of five sampling techniques to estimate surface fuel loading in montane forests**. *International Journal of Wildland Fire*, 17, 363-379. <https://doi.org/10.1071/WF07003>
- Strandberg, J., & Ris, H. (2026). *Utvecklingsplan Alnarpsparken* (Projektnummer 1022649). Ecogain.

- Sun, J.; Qi, W.; Huang, Y., et al. (2023). *Facing the Wildfire Spread Risk Challenge: Where Are We Now and Where Are We Going?* *Fire*, 6(6), 228.
- Thom, D., & Seidl, R. (2016). *Natural disturbance impacts on ecosystem services and biodiversity in temperate and boreal forests*. *Biological Reviews*, 91(3), 760-781. <https://doi.org/10.1111/brv.12193>
- Vanha-Majamaa, I.; Lilja, S.; Ryömä, R., et al. (2007). *Rehabilitating boreal forest structure and species composition in Finland through logging, dead wood creation and fire: The EVO experiment*. *Forest Ecology and Management*, 250(1), 77-88. <https://doi.org/10.1016/j.foreco.2007.03.012>
- Wikars, L.-O. (1997). *Effects of Fire and Ecology of Fire-Adapted Insects*
- WWF. (2020). *Fires, Forests and the Future: A Crisis Raging Out of Control?*
- Ylisirniö, A. L.; Penttilä, R.; Berglund, H., et al. (2012). *Dead wood and polypore diversity in natural post-fire succession forests and managed stands – Lessons for biodiversity management in boreal forests*. *Forest Ecology and Management*, 286, 16-27. <https://doi.org/10.1016/j.foreco.2012.08.018>
- Zhang, Y.; Onda, Y.; Kato, H., et al. (2022). *Understory biomass measurement in a dense plantation forest based on drone-SfM data by a manual low-flying drone under the canopy*. *Journal of Environmental Management*, 312, 114862. <https://doi.org/10.1016/j.jenvman.2022.114862>

Appendix A – Flowchart methodology



Figure 18. Flowchart of the methods divided into 'models' and 'comparison'.

- 1) Preprocessing of LiDAR data into point clouds.
- 2) Slicing points between 0 and 1 metres.
- 3) Calculating the metrics using 6 predictor values: mean height, maximum height, NIR, red, green, blue.
- 4) Generating 2D raster orthophotos.
- 5) Manual selection and classification of reference points.
- 6) Filtering of metrics by the reference points.
- 7) Constructing classification model for deadwood.
- 8) Validation of class-model with accuracy and F1.
- 9) Constructing regression model for green fuels
- 10) Validation of GF-model with R2 and RMSE.

Appendix B – R script classification model

```
library(tidyverse)
library(lidR)
library(terra)
library(sf)
library(raster)
library(randomForest)
library(openxlsx)
library(DHARMA)
library(glmTMB)
library(xfun)
library(pdp)
library(ggplot2)
```

```
#-----#
```

```
# Contents #
```

```
#-----#
```

1. Hagestad

1.1 HA DTM + normalisation

1.2 HA Metrics

1.3 HA Models

1.3.1 GF model

1.3.2 Class model

2. Alnarp park

2.1 AL DTM + normalisation

2.2 AL Metrics

2.3 AL Models

2.3.1 GF model

2.3.2 Class model



Rscript_LiDAR_GFClass.models.pdf

Appendix C – Reference points table

Table 3. Table of reference points in Hagestad, with the coordinates, point ID, presence of deadwood, percentage of green fuel and presence of shade.

X	Y	ID	Deadwood	Green	Shade
14.15736	55.38697	1	1	10	0
14.15736	55.38685	2	0	10	0
14.15706	55.38677	3	1	0	0
14.15742	55.38704	4	0	15	0
14.15735	55.38688	5	1	5	0
14.15709	55.38702	6	1	10	0
14.15681	55.38668	7	0	0	0
14.15694	55.38687	8	1	15	1
14.15688	55.38672	9	1	0	0
14.15731	55.38683	10	1	10	0
14.15707	55.38673	11	0	0	0
14.15744	55.38693	12	0	0	0
14.15692	55.38717	13	0	50	1
14.15695	55.3868	14	1	0	0
14.15728	55.38675	15	0	5	0
14.15725	55.38681	16	0	20	0
14.15721	55.38701	17	1	10	1
14.15741	55.38702	18	0	15	0
14.15715	55.38702	19	0	10	0
14.15681	55.38698	20	1	0	0
14.15695	55.38695	21	0	10	0
14.15713	55.38698	22	0	25	1
14.15693	55.38699	23	1	10	1
14.15723	55.38674	24	0	5	1
14.15732	55.38697	25	1	5	0
14.15674	55.3871	26	0	50	0
14.15726	55.38696	27	1	0	0
14.15717	55.38667	28	1	0	1
14.15692	55.38666	29	1	5	0
14.15727	55.38688	30	0	5	0
14.15698	55.38685	31	1	0	1
14.15731	55.38711	32	1	10	1
14.15742	55.38685	33	0	5	1
14.15735	55.38672	34	0	5	0
14.15682	55.38693	35	1	5	0
14.15734	55.38701	36	0	10	0
14.1568	55.38673	37	1	25	1
14.15731	55.38669	38	1	0	1
14.15694	55.38676	39	1	5	0
14.15748	55.38675	40	0	20	0
14.15689	55.38702	41	0	5	0
14.15713	55.38668	42	0	15	1
14.1568	55.38682	43	1	10	1
14.15683	55.38691	44	0	20	1
14.15722	55.38672	45	0	5	1
14.15756	55.38677	46	0	30	0
14.1572	55.38683	47	0	20	0
14.15684	55.38673	48	0	20	1
14.15683	55.38674	49	1	10	1
14.15676	55.38712	50	1	20	0
14.15674	55.38713	51	0	20	0
14.15674	55.38708	52	0	40	0
14.15675	55.38706	53	0	50	0
14.15677	55.38708	54	0	50	0
14.15715	55.387	55	1	30	1
14.15712	55.387	56	1	30	1
14.15723	55.38706	57	0	20	1
14.15702	55.3872	58	1	20	0
14.15699	55.38722	59	1	40	1
14.15695	55.38721	60	0	50	1

Table 4. Table of reference points in Alnarp, with the coordinates, point ID, presence of deadwood, percentage of green fuel and presence of shade.

X	Y	ID	Deadwood	Green	Shade
13.07481	55.6529	61	1		1
13.07496	55.65302	62	0		0
13.07482	55.65283	63	1		1
13.07468	55.65288	64	0		0
13.07483	55.65303	65	0		0
13.0748	55.65299	66	1		1
13.07467	55.65299	67	0		1
13.07471	55.65292	68	0		1
13.07474	55.65285	69	0		0
13.07485	55.65291	70	0		0
13.07479	55.65282	71	1		1
13.07476	55.65288	72	0		0
13.07471	55.65302	73	0		0
13.0747	55.65295	74	1		1
13.07485	55.65285	75	0		1
13.07485	55.65287	76	0		1
13.07492	55.65301	77	0		0
13.07469	55.65286	78	1		1
13.07492	55.65304	79	0		0
13.0748	55.65294	80	0		1
13.07478	55.65291	81	0		1
13.07492	55.65298	82	1		1
13.07489	55.65294	83	1		1
13.0747	55.65281	84	1		0
13.07472	55.65287	85	1		0
13.07471	55.65297	86	0		1
13.07468	55.6529	87	0		0
13.07486	55.65293	88	0		1
13.07482	55.65285	89	1		0
13.0748	55.65288	90	0		1
13.07472	55.65289	91	1		1
13.07485	55.653	92	1		0
13.07488	55.65303	93	0		0
13.07489	55.65285	94	1		1
13.07481	55.65292	95	1		1
13.07476	55.65289	96	0		1
13.07473	55.65283	97	1		1
13.07485	55.65283	98	0		1
13.07466	55.65294	99	1		1
13.07486	55.65295	100	0		0
13.0749	55.65297	101	0		1
13.07485	55.65289	102	0		0
13.07479	55.65297	103	0		1
13.07467	55.65292	104	0		0
13.07481	55.65281	105	0		1
13.07488	55.653	106	0		1
13.07478	55.65285	107	0		1
13.07471	55.65285	108	0		1
13.07469	55.65283	109	1		1
13.07467	55.65301	110	1		1
13.07468	55.65297	111	0		1
13.07477	55.653	112	1		0
13.07473	55.65293	113	0		1
13.07475	55.65299	114	0		0
13.07498	55.653	115	0		1
13.07475	55.65297	116	1		0
13.07484	55.65298	117	0		1
13.07472	55.65304	118	1		1
13.07468	55.65302	119	1		0
13.07476	55.65304	120	1		1

Publishing and archiving

Approved students' theses at SLU can be published online. As a student you own the copyright to your work and in such cases, you need to approve the publication. In connection with your approval of publication, SLU will process your personal data (name) to make the work searchable on the internet. You can revoke your consent at any time by contacting the library.

Even if you choose not to publish the work or if you revoke your approval, the thesis will be archived digitally according to archive legislation.

You will find links to SLU's publication agreement and SLU's processing of personal data and your rights on this page:

- <https://libanswers.slu.se/en/faq/228318>

YES, I, Lukas van den Elzen, have read and agree to the agreement for publication and the personal data processing that takes place in connection with this

NO, I/we do not give my/our permission to publish the full text of this work. However, the work will be uploaded for archiving and the metadata and summary will be visible and searchable.